

# QUANTUM ENHANCED SENSORS FOR SPACE APPLICATIONS: GOING BEYOND STANDARDS

Savannah L. Cuozzo<sup>1</sup> and Advisor: Eugeny E. Mikhailov<sup>1</sup>

<sup>1</sup>*Department of Physics, College of William & Mary, Williamsburg, Virginia 23187, USA*

(Dated: April 1, 2019)

I report on the controllable response of the lasing frequency to the cavity round-trip path change and how it relates to improved gyroscope sensitivity. By adding an intracavity dispersive medium, I demonstrate a tailorable lasing frequency response with an enhancement up to eight orders of magnitude. This enhancement can be integrated with current navigation technology for a more compact instrument.

Gyroscopes have always played a critical role in spacecraft navigation. Their job is to relay an accurate description of the vehicle's angular direction with respect to an inertial reference frame; without them, pilots would not be able to precisely follow their desired trajectory. Ring laser gyroscopes have been under developed and used as the gyroscopic standard in navigation and fundamental physics since the mid-1900's; clearly, high sensitivity is required.

Laser gyroscopes have a much higher level of precision than mechanical gyroscopes and are significantly more compact, making them more advantageous for space flight. In addition, these gyroscopes have no moving parts and, therefore, require less maintenance and part replacement.

Generally, laser gyroscopes consist of a ring cavity and work by exploiting the Sagnac Effect. Two laser beams are injected into the cavity such that they propagate in opposite directions around the ring cavity. If the ring cavity is rotated clockwise, the laser propagating clockwise will see an effectively longer cavity and the laser propagating counter-clockwise will see an effectively shorter cavity due to the Doppler shift. Since  $f = m\frac{c}{L}$ , where  $f$  is the resonant frequency,  $m$  is the mode number,  $L$  is the total cavity round trip, and  $c$  is the speed of light in vacuum, the change in cavity length corre-

sponds to a change in frequency. When the two beams recombine, they will beat together and their beat note will be directly related to the amount of rotation experienced by the ring cavity.

The response of the beat note to rotations can be enhanced by introducing a dispersive medium into the cavity. By controlling the dispersion, we achieved a  $10^8$  increase of the laser response to the cavity-path length change relative to canonical lasers. The culmination of my research on this subject led to a paper submitted to Physical Review Letters that is now under review (see pages 2-5).

The successful implementation of ultra-high response into laser gyroscopes would enable a new level of precision (potentially 8 orders of magnitude) in gyroscopic measurements that can be seamlessly integrated into NASA's navigation systems used on CubSats, aircraft, and spacecraft, as well as submarines, planes, and defense systems taking up significantly less space and potentially less power to operate.

This would allow for development of smaller, lighter, extremely precise navigation systems that measure the absolute rotation of the object in question. In addition, this work will impact many scientific endeavors, such as furthering the scientific community's understanding of controllable dispersion in active cavities, geodesy, measuring rotation of seismic waves, and general metrology.

# Dispersion enhanced tunability of laser-frequency response to its cavity-length change

Savannah L. Cuzzo<sup>1</sup> and Eugeny E. Mikhailov<sup>1,\*</sup>

<sup>1</sup>*Department of Physics, College of William & Mary, Williamsburg, Virginia 23187, USA*

(Dated: March 12, 2019)

We report on the controllable response of the lasing frequency to the cavity round-trip path change. This is achieved by modifying the dispersion of the intracavity medium in the four-wave mixing regime in Rb. We can either increase the response by a factor of  $10^8$  or drastically reduce it. The former regime is useful for sensitive measurements tracking the cavity round trip length and the latter regime is useful for precision metrology.

PACS numbers: 42.50.Lc, 42.50.Nn

We control the response of the lasing frequency to the laser cavity length change on demand — allowing for either dramatic enhancement or suppression. The resonant frequency link to the cavity round trip path is the foundation for optical precision measurements such as displacement tracking, temperature sensing, optical rotation tracking [1], gravitational wave sensing [2], and refractive index change sensing [3]. In other applications, the laser provides a stable frequency reference, such as precision interferometry [4], optical atomic clocks [5], and distance ranging [6], where the sensitivity of the lasing frequency to the cavity path length change should be reduced. Our findings allow for improved laser assisted precision metrology and potentially make lasers less bulky and immune to the environmental changes in real world applications.

The addition of a dispersive medium to a cavity modifies its frequency response [7] to the geometrical path change ( $dp$ ) according to

$$df_d = -\frac{n}{n_g} \frac{dp}{p_{\text{tot}}} f_0, \quad (1)$$

where  $f_0$  is the original resonant frequency,  $p_{\text{tot}} = p_e + p_d n$  is the total optical round-trip path of the cavity,  $p_d$  is the length of the dispersive element,  $p_e$  is the length of the empty (non-dispersive) part of the cavity,  $n$  is the refractive index, and  $n_g$  is the generalized refractive group index given by

$$n_g = n + \frac{np_d}{p_{\text{tot}}} f_0 \frac{\partial n}{\partial f}. \quad (2)$$

We define the pulling factor (PF) as the ratio of dispersive to empty (non-dispersive,  $n_g = n$ ) cavity response for the same path change

$$\text{PF} \equiv \frac{df_d}{df_e} = \frac{n}{n_g}. \quad (3)$$

The PF is the figure of merit for the enhancement of the cavity response relative to *canonical* lasers or passive cavities operating in the weak dispersion regime with  $n_g = n$ .

We tune the PF by several orders of magnitude in the range from -0.3 to at least  $10^8$  (see Fig. 1), by tailoring

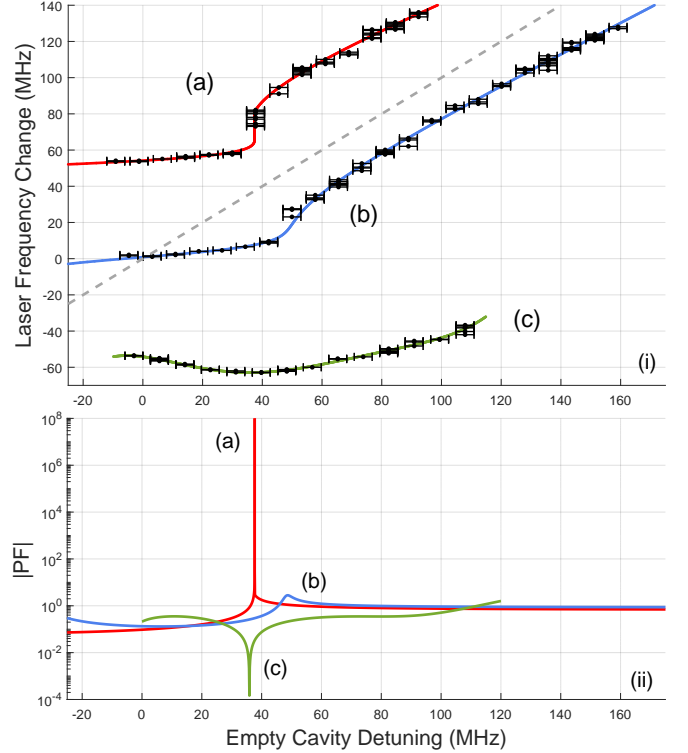


FIG. 1. (Color online) (i) is the experimental lasing frequency dependence on empty cavity detuning (round trip path change) in (a) bifurcating regime with estimated ultra high  $\text{PF} > 10^8$ , (b) high pulling regime with  $\text{PF} = 2.7 \pm 0.4$ , (c) enhanced stability regime where  $|\text{PF}| < 0.2$  crossing 0. The solid lines (a and b) show our best fits of the laser frequency dependence using the model described by Eq. 4; the (c) line is the polynomial fit of the 5th degree. The straight dashed line shows the  $\text{PF} = 1$  dependence (i.e. for an empty cavity). (ii) is the PF calculated based on the fits presented in (i).

the refractive index of our lasing medium. This is the first demonstration of ultra high and tunable PF in the laser.

Due to Kramers-Kronig relationship the negative dispersion is accompanied by local absorption, so it is not surprising that so far the  $\text{PF} > 1$  regime was experimentally demonstrated only in passive, non-lasing cav-

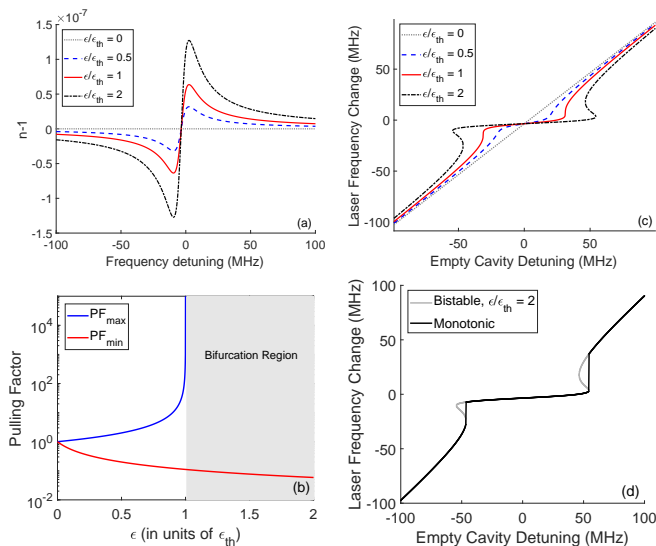


FIG. 2. (Color online) (a) Refractive index change ( $n - 1$ ); (b) dependence of maximum and minimal achievable PF on resonance strength; (c) laser frequency change and (d) bifurcating behavior as functions of detuning (or cavity path change). For all figures  $\gamma$  is set to 6 MHz.

ities [8–10] with  $\text{PF} = 363$ . For active cavities, Yablon *et al.* [11] inferred a  $\text{PF} \sim 190$  via analysis of the lasing linewidth. The increased stability regime ( $\text{PF} < 1$ ) was demonstrated in lasing [12] cavities with the smallest being  $\text{PF} = 1/663$  [13]. Superradiant (“bad-cavity”) lasers, where an atomic gain line is much narrower than a cavity linewidth, exhibit ultra low  $\text{PF} < 10^{-6}$  [14, 15]. Our empty cavity linewidth is about 13 MHz and the atomic gain linewidth is at least 100 MHz (see Fig. 1), so we operate in the “good-cavity” regime unlike work reported in [14, 15].

Similar to [16], we present a simple model of the transmission or amplification spectral line where the index of refraction has the dependence:

$$n(f) = 1 + \epsilon \frac{\gamma \Delta f}{\Delta f^2 + \gamma^2}, \quad (4)$$

where  $\epsilon$  is the resonance strength,  $\Delta f$  is the detuning from the medium resonance frequency ( $f_m$ ), and  $\gamma$  is the resonance width, since  $n(f) - 1 \ll 10^{-5}$  for a vapor filled cavity. For transmission or gain resonances with  $\epsilon > 0$ , the minimum and maximum PF are

$$\text{PF}_{\max} = \frac{1}{1 - \epsilon/\epsilon_{\text{th}}} \quad \text{at} \quad \Delta f = \pm\sqrt{3}\gamma, \quad (5)$$

$$\text{PF}_{\min} = \frac{1}{1 + 8\epsilon/\epsilon_{\text{th}}} \quad \text{at} \quad \Delta f = 0 \quad (6)$$

where

$$\epsilon_{\text{th}} = \frac{8\gamma p_{\text{tot}}}{f_m p_d} \quad (7)$$

is the bifurcating threshold resonance strength.

The analysis of the dispersion (Eq. 4) and its influence on the resonant frequency of the cavity and PF is shown in Fig. 2. As expected, the amplification line has positive dispersion on resonance (see Fig. 2a). Positive dispersion is associated with a large and positive group index, which results in weak dependence (low pulling factor) of the lasing frequency on the cavity path change (empty cavity detuning), as shown in Fig. 2b. Away from resonance, the dispersion is negative leading to high PFs, as shown in Fig. 2b. The stronger the amplification ( $\epsilon$ ) the smaller the  $\text{PF}_{\min}$  is at the center of the resonance, as shown in Fig. 2b. Consequently, the  $\text{PF}_{\max}$  continuously grows and reaches infinity at  $\epsilon = \epsilon_{\text{th}}$  where the resonant frequency bifurcates (see Fig. 2b).

To track dependence of the cavity resonant frequency on the cavity path length, we solve:

$$p_{\text{tot}} = m \frac{c}{f_d}, \quad (8)$$

where  $m$  is the fixed mode number and  $c$  is the speed of light in vacuum. In experiment, it is easier to track the empty cavity detuning (i.e. resonance frequency change,  $\Delta f_e$ ), which is directly linked to the cavity path change via Eq. 1 with  $n_g = n$ . The resulting dependencies are shown in Fig. 2c.

If the negative dispersion is strong enough, the group index could be negative. This would lead to negative PF and to negative dependence of the lasing frequency on the cavity detuning (see line corresponding  $\epsilon = 2\epsilon_{\text{th}}$  in Fig. 2c). This behavior is nonphysical, since it corresponds to a bifurcation [16]: multiple lasing frequencies for the same cavity detuning. Consequently, the laser would ‘jump’ to avoid negative PF region and preserve the monotonic behavior, as shown in Fig. 2d and experimentally in Fig. 1(i)a.

The most important conclusion from the amplifying line analysis is that high pulling (response enhancement) regions exist slightly away from the *gain* resonance. The precursor of such regime is a reduced sensitivity region in close vicinity to the resonance. The off resonance behavior was overlooked in the literature, while it actually provides the road to high PF. Away from the amplification resonance, the system still has enough gain to sustain lasing, and yet it still has large negative dispersion (see Fig. 2a). As detuning from the resonance increases, the dispersion becomes negligible, PF approaches unity (see Fig. 2c and experimental data in Fig. 1 a and b), amplification drops and eventually lasing ceases.

To experimentally demonstrate the modified lasing response to the cavity path change, one needs a narrow gain line to achieve the highest positive dispersion. We utilized the N-level pumping scheme depicted in Fig. 3. The theory and preliminary experimental study of this arrangement are covered in references [12, 17, 18]. The strong pumping field  $\Omega_1$  creates a transmission line for

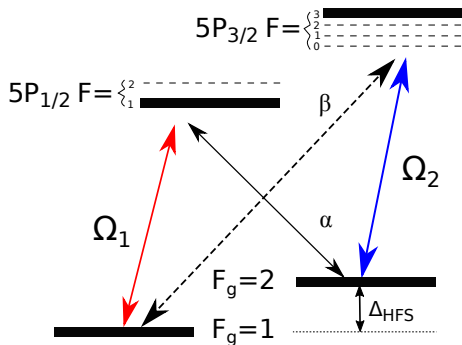


FIG. 3. (Color online) Schematic diagram of interacting light fields and relevant  $^{87}\text{Rb}$  levels.

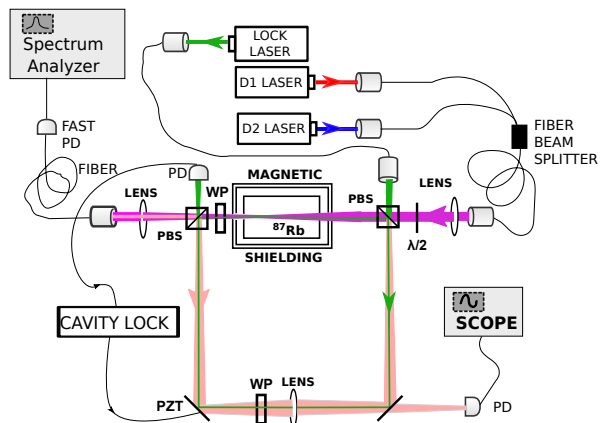


FIG. 4. (Color online) Schematic diagram of the setup. Labels are: PD is photo detector, WP is wave plate,  $\lambda/2$  is half wavelength wave plate, PBS is polarizing beam splitter, and PZT is piezoelectric transducer.

the field  $\alpha$  due to electromagnetically induced transparency. However, the  $\Omega_1$  field alone is not enough to create the amplification. To create the gain for the  $\alpha$  field, we apply another strong repumping field ( $\Omega_2$ ). There is also gain for the  $\beta$  field, which completes the four-wave mixing arrangement of fields  $\Omega_1$ ,  $\Omega_2$ ,  $\alpha$ , and  $\beta$ . But the cavity is tuned to sustain lasing only for  $\alpha$ .

Our lasing cavity is similar to the one used in [12]. The ring cavity is made of two polarizing beam splitters (PBS) and two flat mirrors. The round trip path of the cavity is 80 cm. A 22 mm long Pyrex cylindrical cell with anti-reflection coatings on its windows is placed between the two PBSs and filled with isotopically pure  $^{87}\text{Rb}$ . The cell is encased in a 3-layer magnetic shield and its temperature is set to 100 degrees C. The optical stability of the cavity is increased by adding a 30 cm focal length lens placed between the two mirrors. This lens also places the cavity's mode waist inside the  $^{87}\text{Rb}$  cell.

To produce experimental data sets (a) and (b) shown in the Fig. 1, two pump lasers are tuned near D1 (795 nm) and D2 (780 nm) corresponding to  $\Omega_1$  and  $\Omega_2$  fields in Fig. 3. The pump fields are coupled to a fiber beam

splitter and amplified by a solid state tapered amplifier to powers ranging between 100 mW for set (a) and 170 mW for set (b), and then injected into a ring cavity through a polarizing beam splitter (PBS). The D1 laser is tuned 700 MHz below the  $5S_{1/2}F_g=1 \rightarrow 5P_{1/2}F=1$  transition, and D2 is set to 500 MHz below the  $5S_{1/2}F_g=2 \rightarrow 5P_{3/2}F=3$   $^{87}\text{Rb}$  transition, as seen in Fig. 3. They provide amplification for fields  $\alpha$  and  $\beta$ , which are generated orthogonal to pump fields polarization. Only the  $\alpha$  field resonantly circulates in the cavity, since the pumps exit the cavity via the second PBS and  $\beta$  is kept off-resonance with the cavity.

Since the D1 pump laser is fixed, the beatnote of the pump ( $\Omega_1$ ) and the lasing field ( $\alpha$ ) with its frequency close to  $^{87}\text{Rb}$  hyperfine splitting ( $\Delta_{\text{HFS}} \approx 6.8$  GHz) is related to the frequency of the ring cavity laser and allows us to monitor the dispersive laser frequency change ( $\Delta f_d$ ). We control the cavity length by locking it to an auxiliary laser (called the lock laser) with a wavelength of 795 nm that is far detuned from any atomic resonances and senses a “would be empty” (dispersion-free) cavity detuning ( $\Delta f_e$ ). This lock laser beam counter propagates relative the pump beams and the lasing field to avoid contaminating the detectors monitoring the ring cavity lasing. Two wave plates (WP) are placed inside the cavity. One is to spoil polarization of the lock field and allow it to circulate in the cavity. The other rotates the lasing field polarization by a small amount. This allows it to exit the cavity and mix in with the pump field on the fast photodetector.

The maximum response has the lower bound of  $\text{PF}_{\text{max}} = 1.1 \times 10^8$  at the 90% confidence level for the data set (a), shown in Fig. 1. The upper bound for  $\text{PF}_{\text{max}}$  is infinity since the data set belongs to the bifurcating regime. However, one can smoothly approach this limit by carefully controlling the cavity detuning as our analysis shows in Fig. 1(ii)a. The  $\text{PF}_{\text{min}}$  range is (0.08 to 0.10) for this data set.

We can avoid bifurcation by increasing the pumps' powers (i.e., we increase  $\gamma$  via power broadening), as shown in the data set (b) of Fig. 1. This data demonstrates  $\text{PF}_{\text{max}}$  in the range (2.3 to 3.2). Also, the range of detuning with  $\text{PF} > 1$  is wider. To estimate confidence bounds, we use the modified smoothed bootstrap method [19].

We are able to make our dispersive laser insensitive to its path change, as shown in data set (c) of Fig. 1. We tune the D1 laser to 400 MHz above the  $5S_{1/2}F_g=1 \rightarrow 5P_{1/2}F=1$  transition, and keep D2 at 500 MHz below the  $5S_{1/2}F_g=2 \rightarrow 5P_{3/2}F=3$   $^{87}\text{Rb}$  transition, while maintaining combined pump power at 95 mW. Assuming a smooth dependence on the empty cavity detuning, the PF at the bottom of the U-like curve is exactly zero, as the laser frequency decreases and then increases, while the cavity path (the auxiliary laser detuning) changes monotonically. Our model governed by Eq. 4 cannot ex-

plain the arching behavior, since it does not account for the dependence of the dispersion on the lasing power. However, a more complete model which solves density matrix equations of the N-level scheme predicted such a possibility [12].

There is an ongoing debate whether or not the modified cavity response leads to improved sensitivity (signal to noise ratio) of path-change sensitive detectors. However, laser-based sensors in certain applications might benefit either from enhanced  $PF > 1$  (for example gyroscopes [7]) or reduced  $PF < 1$ , since sensitivity, i.e. the ratio of the response to the lasing linewidth (uncertainty), scales as  $1/PF$  [14, 20]. The tunability and versatility of our system allows to probe either case.

In conclusion, we achieved about  $10^8$  increase of the laser response to the cavity-path length change relative to canonical lasers. We also can significantly reduce the response, making our laser vibration insensitive. These findings broadly impact the fields of laser sensing and metrology, including laser ranging, laser gyroscopes, vibrometers, and laser frequency standards.

EEM and SLC are thankful to the support of Virginia Space Grant Consortium provided by grants 17-225-100527-010 and NNX15AI20H. We would like to thank M. Simons, O. Wolfe, and D. Kutzke for assembling the earlier prototype of our laser. We also thank S. Rochester and D. Budker for their earlier work on N-level theoretical model.

---

\* eemikh@wm.edu

- [1] W. W. Chow, J. Gea-Banacloche, L. M. Pedrotti, V. E. Sanders, W. Schleich, and M. O. Scully, *Rev. Mod. Phys.* **57**, 61 (1985).
- [2] B. P. Abbott and *et al.* (LIGO Scientific Collaboration and Virgo Collaboration), *Phys. Rev. Lett.* **116**, 061102 (2016).
- [3] Y. X. N. Jiyang Li, Haisha Niu, *Optical Engineering* **56**, 050901 (2017).
- [4] D. Martynov and *et al.*, *Phys. Rev. D* **93**, 112004 (2016).
- [5] A. D. Ludlow, M. M. Boyd, J. Ye, E. Peik, and P. O. Schmidt, *Rev. Mod. Phys.* **87**, 637 (2015).
- [6] Y.-S. Jang and S.-W. Kim, *Int. J. Precis. Eng. Manuf.* **18**, 1881 (2017).
- [7] M. S. Shahriar, G. S. Pati, R. Tripathi, V. Gopal, M. Messall, and K. Salit, *Phys. Rev. A* **75**, 053807 (2007).
- [8] G. S. Pati, M. Salit, K. Salit, and M. S. Shahriar, *Phys. Rev. Lett.* **99**, 133601 (2007).
- [9] D. D. Smith, H. A. Luckay, H. Chang, and K. Myneni, *Phys. Rev. A* **94**, 023828 (2016).
- [10] D. D. Smith, H. Chang, P. F. Bertone, K. Myneni, L. M. Smith, and B. E. Grantham, *Opt. Express* **26**, 14905 (2018).
- [11] J. Yablon, Z. Zhou, M. Zhou, Y. Wang, S. Tseng, and M. S. Shahriar, *Opt. Express* **24**, 27444 (2016).
- [12] D. T. Kutzke, O. Wolfe, S. M. Rochester, D. Budker, I. Novikova, and E. E. Mikhailov, *Opt. Lett.* **42**, 2846 (2017).
- [13] J. Yablon, Z. Zhou, N. Condon, D. Hileman, S. Tseng, and S. Shahriar, *Opt. Express* **25**, 30327 (2017).
- [14] J. G. Bohnet, Z. Chen, J. M. Weiner, D. Meiser, M. J. Holland, and J. K. Thompson, *Nature* **484**, 78 (2012).
- [15] M. A. Norcia, J. R. K. Cline, J. A. Muniz, J. M. Robinson, R. B. Hutson, A. Goban, G. E. Marti, J. Ye, and J. K. Thompson, *Phys. Rev. X* **8**, 021036 (2018).
- [16] Z. Zhou, J. Yablon, M. Zhou, Y. Wang, A. Heifetz, and M. Shahriar, *Optics Communications* **358**, 6 (2016).
- [17] E. E. Mikhailov, J. Evans, D. Budker, S. M. Rochester, and I. Novikova, *Optical Engineering* **53**, 102709 (2014).
- [18] N. B. Phillips, I. Novikova, E. E. Mikhailov, D. Budker, and S. Rochester, *Journal of Modern Optics* **60**, 64 (2013), [arXiv:1205.2567](https://arxiv.org/abs/1205.2567).
- [19] B. Efron and R. Tibshirani, *An Introduction to the Bootstrap* (Chapman and Hall/CRC, 1994).
- [20] C. Henry, *IEEE Journal of Quantum Electronics* **18**, 259 (1982).